

PPAR Signaling Pathway and Cancer-Related Proteins Are Involved in Celiac Disease-Associated Tissue Damage

Maria Paola Simula,¹ Renato Cannizzaro,² Vincenzo Canzonieri,³ Alessandro Pavan,¹ Stefania Maiero,² Giuseppe Toffoli,¹ and Valli De Re¹

¹Experimental and Clinical Pharmacology Unit, ²Department of Gastroenterology, and ³Department of Pathology, CRO Centro di Riferimento Oncologico, IRCCS National Cancer Institute, AVIANO (PN), Italy

Celiac disease (CD) is an immune-mediated disorder triggered by the ingestion of wheat gliadin and related proteins in genetically predisposed individuals. To find a proteomic CD diagnostic signature and to gain a better understanding of pathogenetic mechanisms associated with CD, we analyzed the intestinal mucosa proteome alterations using two dimensional difference gel electrophoresis (2D-DIGE) coupled with matrix assisted laser desorption ionization time of flight mass spectrometry (MALDI-TOF ms) of CD patients with varying degrees of histological abnormalities defined by Marsh criteria and controls. Our results clearly evidenced the presence of two groups of patients: Group A, including controls and Marsh 0-I CD patients; and Group B, consisting of CD subjects with grade II-III Oberhuber-Marsh classification. Differentially expressed proteins were involved mainly in lipid, protein and sugar metabolism. Interestingly, in Group B, several downregulated proteins (FABP1, FABP2, APOC3, HMGCS2, ACADM and PEPCK) were implicated directly in the peroxisome proliferator-activated receptor (PPAR) signaling pathway. Moreover, Group B patients presented a deregulation of some proteins involved in apoptosis/survival pathways: phosphatidylethanolamine-binding protein 1 (PEBP1), Ras-related nuclear protein (Ran) and peroxiredoxin 4 (PRDX4). PEBP1 downregulation and RAN and PRDX4 upregulation were associated with more severe tissue damage. Likewise, IgMs were found strongly upregulated in Group B. In conclusion, our results indicate that a downregulation of proteins involved in PPAR signaling and the modulation of several cancer-related proteins are associated with the highest CD histological score according to Oberhuber-Marsh classification.

© 2010 The Feinstein Institute for Medical Research, www.feinsteininstitute.org

Online address: <http://www.molmed.org>

doi: 10.2119/molmed.2009.00173

INTRODUCTION

Celiac disease (CD) is caused by an immune reaction to gliadin, a gluten protein found in wheat gluten and related derivatives, in genetically predisposed individuals. The main histological feature of CD is represented by the presence of a chronic inflammation of the small bowel's mucosa and submucosa (1,2), which produces extremely polymorphic clinical manifestations ranging from severe chronic enteritis and malabsorption to diarrhea, constipation, flatulence, weight loss, vitamin and mineral deficiencies, iron deficiency and bone dis-

ease. However in some cases, there are no gastrointestinal symptoms (3), or they are less pronounced. A permanent gluten-free diet (GFD) is currently the only accepted therapy for CD. Although most individuals respond to treatment, a minority of them ($\leq 5\%$) may have persistent symptoms and villous atrophy despite scrupulous adherence to a GFD: this disorder is called refractory CD (RF-CD). The prognosis of this subgroup of patients is poor, and they show a higher risk of developing an overt lymphoma and uncontrolled malabsorption. Moreover, overall CD patients present a

higher risk of developing cancer (4,5). Cancers include T- and B-cell non-Hodgkin lymphoma, oropharyngeal, esophageal and intestinal adenocarcinomas and pancreas tumors (6).

In most patients, the CD diagnosis is easily established. Nevertheless, roughly 10% of cases are difficult to diagnose because of a lack of concordance among serologic, clinical and histologic findings. The diagnosis of latent CD is usually retrospective and it is difficult to interpret whether minor small bowel mucosal changes are due to early developed CD or whether the infiltrative lymphoid cells represent an unspecific finding (7). Thus, there are a substantial number of latent and undiagnosed cases (8).

In CD, immune responses to gliadin promote the inflammatory reaction, primarily in the upper small intestine, characterized by the infiltration of the lamina propria and the epithelium with chronic

Address correspondence and reprint requests to Valli De Re, Experimental and Clinical Pharmacology Unit, CRO Centro di Riferimento Oncologico, IRCCS National Cancer Institute, via F. Gallini 2, 33081 AVIANO (PN) Italy. Phone: + 39-0434-659672-829; Fax: + 39-0434-659799; E-mail: vdere@cro.it.

Submitted November 22, 2009; Accepted for publication March 2, 2010; Epub (www.molmed.org) ahead of print March 3, 2010.

inflammatory cells and villous atrophy. It is known that acquired T cell-mediated and innate immune mechanisms have an important role in CD pathogenesis (9). T cell-mediated adaptive response is mediated by CD4 + TH1 lymphocytes in the lamina propria that recognize deamidated gliadin peptides, bound to DQ2 or DQ8 HLA-II molecules, on antigen-presenting cells; T cells subsequently produce proinflammatory cytokines (10), mainly interferon (IFN)- γ (11). Tissue transglutaminase (TG2) is the enzyme that deamidates gliadin peptides determining the immunostimulator effect of gluten (12). Additional functions of TG2 consist of cross-linking gluten peptides, thus forming supramolecular complexes contributing to the formation of a wide range of T cell-stimulatory epitopes that might be implicated in different stages of the disease formation; in this context, the α 2-gliadin-33mer fragment is the most immunogenic because it harbors six partly overlapping DQ2-restricted epitopes (13). The ensuing inflammatory cascade releases metalloproteinases and other tissue-damaging mediators that induce crypt hyperplasia and villous injury (14). Moreover, gliadin peptides can elicit innate immune responses that, in concert with adaptive immunity, induce mucosal damage via a T-independent pathway. In particular, it was shown that gluten peptides elicit an increased expression of interleukin-15 by macrophages, epithelial cells and dendritic cells in the lamina propria, that results in the activation of intraepithelial lymphocytes expressing the natural-killer (NK) activating receptors CD94 and NK-G2D (15,16). These activated cells become cytotoxic and kill enterocytes expressing the NK-G2D ligand, the major-histocompatibility-complex class I chain related A (MIC-A), a cell-surface antigen induced by cellular stress, thus contributing to enhanced enterocyte apoptosis (6,17,18). Upregulation of IL-15 expression by epithelial cells and dendritic cells in the lamina propria seems to also contribute to the altered signaling properties of the CD8+ T cell population (16). In addition, recent ge-

nome-wide association studies have provided convincing evidence that the *IL-21* gene also is associated with CD (19,20). *IL-21* has been shown to stimulate epithelial cells to secrete chemokines, to facilitate the recruitment of immune cells within the inflamed tissue and to modulate the proliferation and function of CD8 + T and NK cells (21). Moreover, in its role in the control of B-cell and plasma cell function, *IL-21* may also contribute to the production of CD-associated anti-transglutaminase autoantibodies (22). These observations collectively underline the complexity of the CD pathogenesis and suggest the activation of multiple cellular pathways.

Proteomic analysis is a promising tool to enhance our knowledge of fundamental aspects of how the biological systems operate and to provide practical insights that will impact medical practice (23,24). To gain a better understanding of pathogenetic mechanisms associated with CD, we used a combination of proteomic technologies: two dimensional difference gel electrophoresis (2D-DIGE) coupled with matrix assisted laser desorption ionization time of flight mass spectrometry (MALDI-TOF ms), to investigate the intestinal mucosa tissue proteome alterations of CD patients, with respect to controls.

Our results highlight the downregulation of proteins involved in the PPAR pathway and the modulation of some cancer-related proteins associated with the highest histological grade of CD.

MATERIALS AND METHODS

Patients

For proteomic analysis, duodenal biopsies were obtained from 19 suspected adult CD patients attending the Centro di Riferimento Oncologico in Aviano, Italy. Biopsies were fixed in Bouin solution and a portion of unfixed tissue was snap frozen in liquid nitrogen and stored at -80°C . Histological evaluation was performed according to modified Oberhuber-Marsh classification (2). HLA DQB1 typing was carried out as reported previously (25).

Molecular, immunohistochemical and serologic analyses excluded a CD diagnosis for 7/19 patients who were used as controls (Table 1); 10/19 subjects were confirmed to be positive for CD and the remaining 2/19 were suspected CD patients. Among confirmed CD patients, two have a Marsh 0, two a Marsh I, one has a Marsh II and five have a Marsh III histological classification. HLA DQ2/8 variants were present in all CD patients, in the suspected CD patients and in two patients with excluded CD.

Among CD patients, two were under GFD while the remaining cases were CD at first diagnosis (Table 1). Five patients with refractory CD (RF-CD) who no longer respond to a GFD (Table 1) have been analyzed by immunoblotting. All patients have been notified of the purpose of the study and an informed consent has been obtained for all participants.

Sample Preparation and 2D-DIGE Analysis

2D-DIGE analysis was carried out as reported previously (26,27). Proteins were extracted from gut biopsies with a sample grinding kit (GE Healthcare, Uppsala, Sweden) and 200 μL of lysis buffer (7 mol/L urea, 2 mol/L thiourea, 4% CHAPS and 30 mmol/L Tris-HCl pH 8.5). The cell lysates were precipitated before 2D-DIGE using a 2-D Clean-Up kit (GE Healthcare) and then resuspended in 7 mol/L urea, 2 mol/L thiourea and 4% CHAPS. Protein concentration was determined with Bio-Rad protein assay (Bio-Rad, Milan, IT). For DIGE minimal labeling, 25 μg of protein sample were mixed with 100 pmol CyDye (GE Healthcare). Then the sample pairs were mixed with the internal standard following the experimental design reported in Table 2. The internal standard, including equal amounts of all the samples within the experiment, has been labeled with Cy2 dye. We also adopted a dye swapping strategy to avoid a dye labeling bias, therefore Cy3 and Cy5 dyes were interchangeable.

Eleven-cm immobilized pH gradient strips (pH 3–10 NL) (Bio-Rad) were rehy-

Table 1. Patients characteristics.

Patient	Age/Sex	DQ2/8 variant	Modified MARSH grade	Celiac disease	Group	Diagnosis/diet (months)	Anti-Transglutaminase ^a	CD familiarity
CD patients								
Patient 1	26/M	- ^b	0	Excluded	Group A	0/0	-/-	
Patient 2	42/F	-	0	Excluded	Group A	0/0	-/-	
Patient 3	16/F	DQ2	0	Excluded	Group A	0/0	-/-	
Patient 4	19/F	-	0	Excluded	Group A	0/0	31/-	yes
Patient 5	59/F	DQ2	0	Excluded	Group A	0/0	31/-	
Patient 6	25/M	-	0	Excluded	Group A	0/0	37/-	
Patient 7	34/F	-	0	Excluded	Group A	0/0	52/-	
Patient 8	44/M	DQ2	0	Suspected ^c	Group A	36/36	-/-	
Patient 9	46/M	DQ2	0	Suspected ^d	Group A	0/0	-/7.5	
Patient 10	39/F	DQ2	0	Confirmed	Group A	0/0	-/16	
Patient 11	22/F	DQ2	0	Confirmed	Group A	0/0	-/73	yes
Patient 12	47/F	DQ2	I	Confirmed	Group A	60/58	-/-	
Patient 13	34/M	DQ2	I	Confirmed	Group A	25/24	-/08	
Patient 14	39/F	DQ2	II	Confirmed	Group B	0/0	26/16	
Patient 15	52/M	DQ2	III A	Confirmed	Group B	0/0	-/15	
Patient 16	36/M	DQ2	III B	Confirmed	Group B	0/0	26/20	
Patient 17	41/M	DQ2	III B	Confirmed	Group B	0/0	-/21	
Patient 18	38/F	DQ2	III A	Confirmed	Group B	0/0	130/NE ^e	
Patient 19	33/F	DQ2	III A	Confirmed	Group B	0/0	336/NE	
Refractory CD patients								
Patient 20	32/F	DQ2	III B	Confirmed		96/72	-/-	yes
Patient 21	29/F	DQ8	III A	Confirmed		12/12	-/-	
Patient 22	43/F	DQ2	III A	Confirmed		120/118	-/-	
Patient 23	41/M	DQ2	III A	Confirmed		240/238	-/-	
Patient 24	32/F	DQ2 and DQ8	III A	Confirmed		60/57	400/400	

^aDashes indicate values lower than the cutoff.

^bDashes indicate patient does not carry either variant.

^cPatient with ulcerative jejunoileitis.

^dPatient with pancreatic cysts and intraductal tumor.

^eNE: not evaluated.

drated passively overnight and then run on a Bio-Rad Protean IEF Cell. The following voltage program was used for first dimension separation: 250 V for 15 min, a slow voltage ramp to 8,000 V over 2.5 h

and a final focusing step for a total of 35,000 Vh. Focused IPG strips were stored at -80°C before equilibration and application to SDS-PAGE. For the second dimension, IPG strips were equilibrated in

7 mol/L urea, 2 mol/L thiourea, 2% SDS, 30% glycerol and 50 mmol/L Tris-HCl pH 8.8, reduced with 65 mmol/L DTT and alkylated with 135 mmol/L iodoacetamide. The second dimension was run on Criterion IPG + 1 Comb 8-16% precast gels (Bio-Rad). Gels were scanned on a Typhoon TRIO scanner (GE Healthcare) at 100 mm resolution (emission filters centered at 520 nm, 580 nm and 670 nm for Cy2, Cy3 and Cy5 respectively). Images were subjected to Biological Variation Analysis (BVA), allowed matching of spots from multiple gels; then, the Difference In-gel Analysis (DIA) (using DeCyder software version 6.5 [GE Healthcare]) normalized, and statistically analyzed spot abundance to identify and quantify differentially expressed proteins. The Ex-

Table 2. 2D-DIGE experimental design.

Gel number	Cy2	Cy3	Cy5
1	Pooled standard	Control	CD Marsh I
2	Pooled standard	CD Marsh III B	Control
3	Pooled standard	Control	-
4	Pooled standard	Suspected CD Marsh 0	Suspected CD Marsh 0
5	Pooled standard	CD Marsh I	CD Marsh III A
6	Pooled standard	CD Marsh III A	Control
7	Pooled standard	Control	CD Marsh 0
8	Pooled standard	CD Marsh III A	CD Marsh II
9	Pooled standard	CD Marsh 0	Control
10	Pooled standard	Control	CD Marsh III B

tended Data Analysis (EDA) module was used for multivariate analysis of protein expression data, derived from the BVA and DIA modules through principal component analysis (PCA), pattern analysis and discriminant analysis.

Protein Identification by MALDI-TOF Peptide Mass Fingerprinting

Preparative gel was obtained by the above described procedure, with a 300 µg total protein load. After 2-DE, the gel was fixed in 50% ethanol and 2% orthophosphoric acid followed by an exposure to a staining solution (17% $[\text{NH}_4]_2\text{SO}_4$, 2% orthophosphoric acid, 34% methanol). Coomassie Colloidal G-250 was added to a final concentration of 0.065%. Destaining of the gel was performed with deionized water until the background was completely clear. Coomassie-stained gel was scanned with a GS-800 densitometer (Bio-Rad) at 63 µm resolution. Protein spots of interest were excised from the preparative gel and destained with 25 mmol/L ammonium bicarbonate in 50% acetonitrile. After overnight trypsin digestion, peptides were extracted with 1% TFA, subjected to Zip Tip cleanup (Millipore, Milan, IT), and directly eluted with an α -Cyano-4-hydroxycinnamic acid matrix (10 g/L α -Cyano-4-hydroxycinnamic acid in 50% acetonitrile and 0.3% TFA). Peptide mass fingerprinting (PMF) was performed on a Voyager-DE PRO Biospectrometry Workstation mass spectrometer (Applied Biosystems, Foster City, CA, USA). MALDI-TOF mass spectra were acquired in 700–4,000 Da molecular weight range, in reflector and in positive-ion mode, with 150 nanosecond delay time and an ion acceleration voltage of 20 kV. Spectra were calibrated externally using Peptide calibration Mix 4, 500-3500 Da (Laser Bio Labs, Nice, France). Mass spectra, obtained by collecting 1,000–2,000 laser shots, were processed using Data Explorer version 5.1 software (Applied Biosystems). Peak lists have been obtained from the raw data following advanced baseline correction (peak width 32, flexibility 0.5, degree 0.1), noise filtering (noise filter correlation factor 0.7) and

monoisotopic peak selection. Database search was done with the online MASCOT search engine (<http://www.matrixscience.com>), Aldente (<http://www.expasy.org/tools/aldente>) and ProFound (<http://prowl.rockefeller.edu/prowl-cgi/profound.exe>) PMF tools, against the NCBI nr and Swiss Prot databases, limiting the search to human proteins, allowing for one trypsin missed cleavage and with a 100 ppm mass tolerance error. The fixed modification selected was cysteine carbamidomethylation, while the variable modification selected was the methionine oxidation. The protein list has been analyzed with the Pathway Express tool (<http://vortex.cs.wayne.edu/projects.htm>) (28) to find all associated pathways.

Immunoblotting Analysis

For Western blot analysis, 25 mg of protein extracts, each comprising equal amounts of proteins from patient's Group A and B, were run on 4% to 20% gradient precast gels (Bio-Rad) and transferred onto Protran Nitrocellulose Transfer membrane (Schleicher-Schuell, Dassel, DE, Germany) using Trans Blot Semi-dry Transfer cell (Bio-Rad) (29). The membranes were blocked with 2% nonfat milk. The primary antibodies used were: mouse antihuman RAN monoclonal antibody (1:3000) (clone ARAN1, Novus Biologicals, Littleton, CO, USA); polyclonal goat antihuman IgM HRP conjugated (1:1000) (Sigma, St. Louis, MO, USA); rabbit anti-PEBP1 polyclonal antibody (1:1000) (Cell Signaling, Danvers, MA, USA), goat polyclonal anti-FABP antibody (1:1000) (clone C-20, Santa Cruz, CA, USA); and goat antivinculin polyclonal antibody (1:1000) (clone N-19, Santa Cruz), that was used as control for equal loading. Secondary antibodies were goat antimouse IgG (1:1000) (GE Healthcare), goat antirabbit IgG (1:1000) (Cell Signaling) and donkey antigoat IgG (1:5000) (Santa Cruz), all HRP conjugated. Detection of immunoreactive proteins was accomplished with ECL Western blot detection reagent (GE Healthcare) followed by autoradiography with Hyperfilm ECL (GE Healthcare).

The same experimental procedure has been used to determine the expression levels of RAN, IgM, FABP and RKIP in patients with RF-CD. Twenty-five micrograms of protein extracts from patients 1, 2 and 3, representing the controls; 16, 17 and 19, belonging to CD patients Group B; and patients 20–24, representing the group of subjects with RF-CD, were individually loaded and run on 4% to 20% gradient precast gels and then processed as described above.

The bands were quantified by densitometry, with a GS-800 densitometer (Bio-Rad) and Quantity One software v.4.5, to obtain an integral volume value (optical density, OD × area), which was then normalized with respect to the vinculin value.

RESULTS

Analysis of CD Proteins by 2D-DIGE

PCA analysis and hierarchical clustering. The first analysis was performed following classification criteria based on histological Marsh grades of bioptic samples. Patients were, in turn, grouped as with pre-infiltrative (Marsh 0), infiltrative (Marsh I), infiltrative-hyperplastic (Marsh II) and destructive (Marsh III) lesions. Following the differential expression analysis, we created a set comprised of proteins present in more than 80% of spot maps and with a one-way analysis of variance (ANOVA) $P < 0.01$. Results from principal component analysis (PCA) evidenced the presence of only two groups with relevant biological correlation between proteins expression and Marsh classification: controls and CD patients with Marsh 0–I on one side (Group A) and CD patients with Marsh II–III on the other side (Group B). The same results were obtained when algorithm hierarchical clustering and pattern analysis were performed. All the subsequent calculations were then carried out following the above-described partition. PCA and hierarchical clustering were repeated, including proteins present in more than 80% of the spot maps and with a Student t test ($P < 0.05$) (Figure 1).

Differentially expressed proteins. Differential expression analysis between

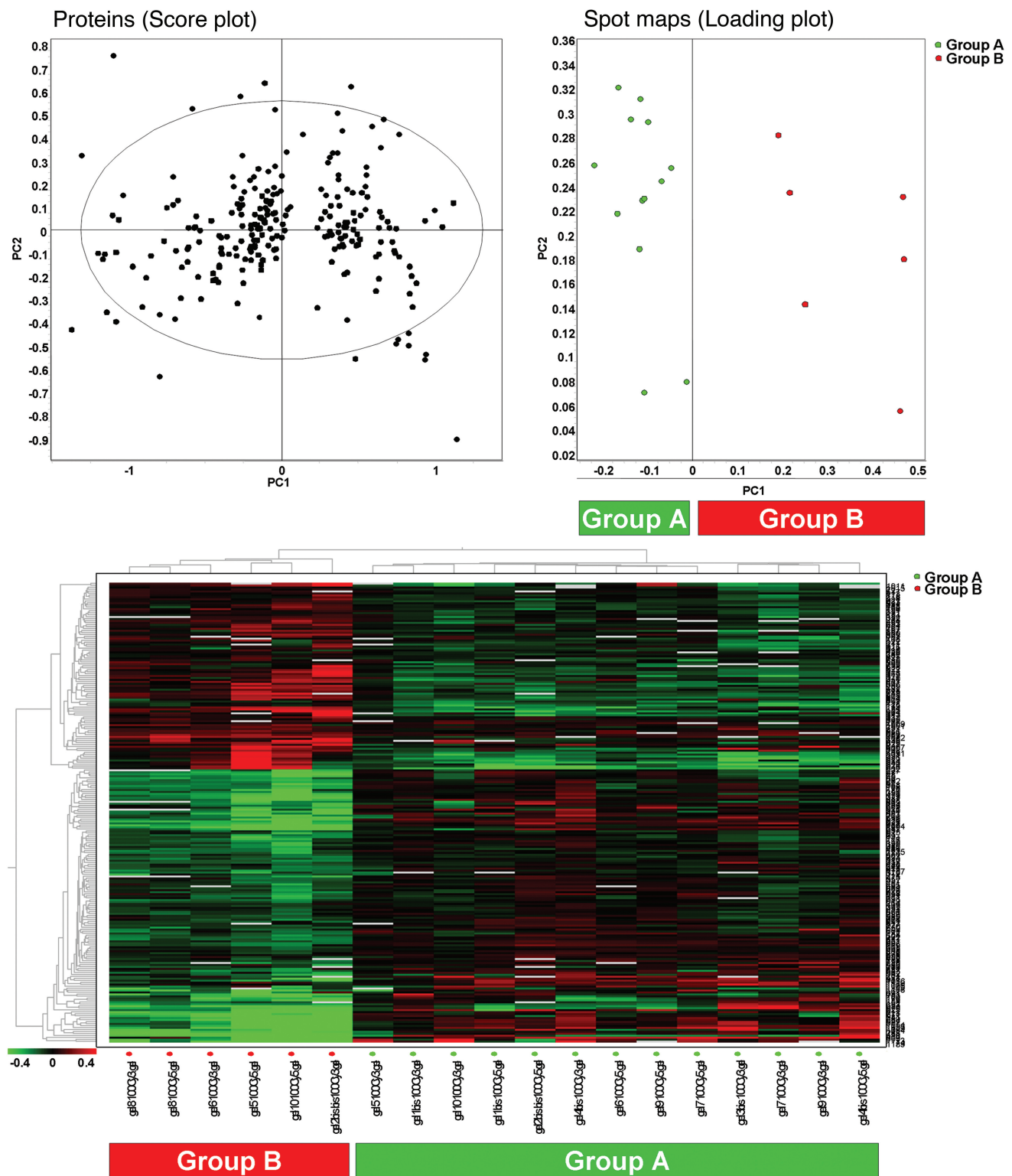


Figure 1. Principal component and pattern analyses of protein maps from controls and CD patients with Marsh 0-I (Group A) and CD patients with Marsh II-III (Group B). We performed PCA and hierarchical clustering on a set comprising proteins present in more than 80% of spot maps and with a *t* test *P* < 0.05.

Group A and B evidenced 234 significantly modulated proteins. The most significant ones (80 spots, $P < 0.01$) were excised from the Coomassie stained preparative gel and then identified by MALDI-TOF PMF. The protein identification was obtained successfully in 54 of the 80 excised spots. A comprehensive list of all identified proteins is reported in Table 3 (30). Differentially expressed proteins, marking Group A with respect to Group B, were involved mainly in several metabolic pathways: glycolysis/ gluconeogenesis, lipid, glycerolipid and glycerophospholipid metabolism, urea cycle, metabolism of amino groups, metabolism of nitrogenous molecules, protein synthesis and degradation and purine metabolism (Table 3).

Of note, we found that, in Group B, several downregulated proteins (FABP1, FABP2, APOC3, HMGCS2, ACADM, PEPCK) were implicated directly in the PPAR signaling pathway as resulting from Pathway Express tool analysis ($P = 1.62e-8$; Figure 2) (28).

In addition, Group B patients presented a deregulation of some proteins involved in apoptosis/survival pathways: phosphatidylethanolamine-binding protein 1 (PEBP1), also known as Raf kinase inhibitory protein (RKIP), Ras-related nuclear protein Ran and peroxiredoxin 4 (PRDX4). Among them, PEPB1 and RAN proteins, respectively down- and upregulated in Group B, were particularly interesting for their involvement in cancer development.

Finally, we found that IgMs were upregulated strongly in patients with the highest histological grade of CD (Group B).

Marker selection. The EDA discriminant analysis tool can be used to find the smallest subset of proteins, called classifiers, that allows distinguishing between experimental groups and eventually classify a new set of spot maps.

Marker selection calculation was performed with the set including proteins present in more than 80% of spot maps and with a *t* test ($P < 0.05$). Analysis was performed with partial least squares method as search method, and with reg-

ularized discriminant analysis as evaluation method. As cross-validation options, we set five folds.

Results indicated that using two of the proteins indicated in Table 4, the IgM, selected by all the classifiers and fatty acid binding protein, chosen by two out of five classifiers, it is possible to discriminate between Group A and B with an accuracy score of 100% (data not shown). We created a classifier, identified as RDA1, comprised of IgM and fatty acid binding protein. This classifier was able to classify all the analyzed samples correctly.

Immunoblotting Analysis

We have used the protein immunoblotting assay to confirm the differential expression of IgM, FABP, RAN and PEBP1 in the two groups of patients. Vinculin has been used as control for equal loading. Figure 3 shows the immunoblotting results. Normalizing the Western blot results against vinculin, we confirmed that IgM and RAN were upregulated, while PEBP1 and FABP were downregulated in Group B, in accordance with 2D-DIGE analysis.

We therefore examined the expression level (mean \pm SD) of these proteins, normalized with respect to vinculin, on patients with RF-CD. As a preliminary result from RF-CD patients, tissue IgM level remained elevated with respect to controls (2.3 ± 1.01 versus 1.4 ± 0.1), FABP decreased in Group B patients, but reversed toward normalization in RF-CD patients (0.9 ± 0.6 versus 0.8 ± 0.1), RAN was increased further (1.9 ± 0.6 versus 1.2 ± 0.3) while PEBP1 was decreased (1.6 ± 0.9 versus 2.7 ± 0.7) (Figure 3).

DISCUSSION

CD occurs in adults and children at rates approaching 1% of the population (6,31,32). Its diagnosis requires abnormalities on laboratory tests that might be caused by malabsorption (for example, folate deficiency and iron-deficiency anemia), the presence of high antigliadin titers, antitissue transglutaminase and antiendomysial antibodies, the presence of an HLA DQ2/8 variant, a duodenal

biopsy that shows the characteristic findings of intraepithelial lymphocytosis, crypt hyperplasia, villous atrophy and, above all, a positive response to a gluten free diet (GFD). The spectrum of pathologic changes in CD ranges from near-normal villous architecture, with a prominent intraepithelial lymphocytosis, to total villous atrophy (33).

The histologic findings in CD are characteristic but not specific (34); their presence, and particularly the observation of a Marsh-Oberhuber type III lesion, permits a presumptive diagnosis of CD and initiation of a GFD. CD is not the only cause of lymphocytosis and villous atrophy (35) and the diagnosis is confirmed only when there is a favorable response to the diet, evaluated after at least a 6-month follow up. Moreover, the pathogenesis of CD-associated tissue damage is still poorly understood (36).

On these grounds, the aim of this study was to investigate for the first time the intestinal mucosa tissue proteome alterations between CD patients with different histological Marsh grade and a control group of patients in whom a CD diagnosis was excluded after clinical, laboratory and histological examinations.

The comparison of the protein expression profile of CD patients grouped according to their histological classification and controls, by both PCA and pattern analyses, failed in discriminating between latent or non-specific forms (Marsh 0-I) and controls. By converse, it clearly emerged that a common protein profile characterized the patient with an infiltrative-hyperplastic (Marsh II) and the patients with a destructive (Marsh III) lesion. Following a two-group classification scheme, Group A (controls and CD patients with Marsh 0-I) and Group B (CD patients with Marsh II-III), the combination of 2D-DIGE, DeCyder EDA and MALDI-TOF PMF, led us to achieve a classifier (Table 4), composed by two proteins (IgM and FABP1) that was able to distinguish between these two groups with 100% accuracy.

Among the proteins included in the classifiers, the IgM upregulation repre-

Table 3. Identified differentially expressed proteins.

Protein name	Average ratio ^a	DeCyder P value ^b	Spot ^c	Database accession number ^d	MW (kDa)	pI	Matching peptides	Coverage (%)	Identification P value
Ig mu chain C region	2.92	1.93e-4	224	P01871	50	6,4	11	19	1,00E-04
	3.71	1.18e-4	227				10	22	1,20E-02
PPAR signaling pathway									
Phosphoenolpyruvate carboxykinase	-2.92	1.96e-4	288	Q16822	71	7,5	17	22	3,20E-08
	-3.3	3.55e-5	289				19	27	1,00E-08
Hydroxymethylglutaryl-CoA synthase	-3.33	4.49e-6	436	P54868	55	8,7	12	16	1,60E-05
Medium-chain specific acyl-CoA dehydrogenase	-1.52	4.01e-4	476	P11310	47	8,6	15	31	8,10E-07
Fatty acid binding protein	-4.23	2.91e-5	1094	P12104	15	6,6	7	31	1,90E-02
Fatty acid-binding protein	-3.1	3.16e-4	1123	P07148	14	6,6	6	38	3,30E-02
Apolipoprotein C3	-4.22	1.66e-4	1189	P02656	9	4,7	4	46	9,20E-04
Carbonyl reductase (NADPH) 1	-1.71	4.65e-7	669	P16152	31	8,6	18	72	1,00E-20
	-2.77	4.65e-7	683				13	43	1,00E-06
Retinol binding protein II	-2.99	1.12e-4	1054	P50120	16	5,3	7	42	2,60E-02
	-2.72	1.93e-4	1057				5	35	1,40E-02
Protein metabolism									
Carbamoyl-phosphate synthase	-1.92	7.56e-5	48	P31327	166	6,3	9	5	3,20E-02
	-2.03	8.78e-5	49				16	9	5,10E-06
	-1.76	1.93e-4	56				32	22	2,60E-19
Elongation factor 2	1.53	4.84e-4	134	P13639	96	6,4	16	16	1,00E-08
Tryptophanyl-tRNA synthetase	2.04	1.45e-4	377	P23381	53	5,8	16	28	1,00E-09
Ornithine aminotransferase	-1.84	8.78e-5	479	P04181	49	6,6	10	22	1,90E-04
Aminoacylase-1	-2.07	7.36e-6	487	Q03154	46	5,8	16	38	6,40E-10
Ornithine aminotransferase	-2.27	2.84e-5	488	P04181	49	6,6	16	33	1,00E-09
Ornithine carbamoyltransferase	-2.08	1.14e-4	563	P00480	36	7,9	12	20	1,50E-04
Proteasome subunit α type-6	1.37	1.41e-3	797	P60900	28	6,3	9	32	5,90E-04
Sugar metabolism									
Sucrase	-1.72	8.48e-5	62	P14410	210	5,4	22	11	6,40E-06
	-3.43	7.31e-6	67				20	9	3,20E-07
Fructose biphosphate aldolase B	-3.2	3.55e-5	554	P05062	40	8,3	13	29	6,70E-04
Aldose 1-epimerase	-1.57	1.92e-6	581	Q96C23	38	6,2	8	30	1,80E-04
Fructose-1,6-bisphosphatase	-2.96	2.15e-6	582	P09467	37	6,5	16	33	3,20E-13
Aflatoxin B1 aldehyde reductase member 3	-1.37	5.91e-4	620	O95154	37	6,7	14	41	3,20E-07
Lipid metabolism									
Aldo-keto reductase family 1 member B10	-2.97	3.13e-3	605	O60218	36	7,1	7	20	2,50E-02
	-2.31	2.34e-4	615				11	32	4,70E-04
Glycerol-3-phosphate dehydrogenase	-2.39	5.39e-6	623	P21695	38	5,8	11	22	8,00E-07
Hydroxyacyl-coenzyme A dehydrogenase	-1.62	1.04e-4	665	Q16836	33	8,4	14	30	3,20E-07
Dihydroxyacetone kinase	-2.03	2.20e-5	323	Q3LXA3	59	7,6	15	30	3,20E-09
Energy production									
Aconitate hydratase	-1.74	8.48e-5	180	Q99798	86	7,6	22	28	8,10E-09
Cytochrome b5	-2.4	1.57e-5	1004	P00167	11	5	7	79	2,50E-08
Detoxification									
Catalase	-1.39	1.00e-4	337	P04040	60	6,9	15	28	1,60E-08
Sulfotransferase 1A3/1A4	-1.92	1.50e-4	643	P50224	34	5,7	16	56	1,30E-11
Glutathione S-transferase A1	-1.96	3.16e-4	820	P08263	26	8,9	7	21	1,20E-02

Continued

Table 3. Continued.

Cell proliferation/apoptosis										
GTP-binding nuclear protein Ran	1.91	2.67e-6	814	P62826	25	7,1	11	42	1,30E-08	
Phosphatidylethanolamine-binding protein 1	-1.42	1.25e-3	882	P30086	21	7,4	12	56	1,30E-07	
Hypotetical protein MGC29506	2.61	3.22e-5	964	Q8WU39	21	5,4	8	28	3,80E-02	
Peroxiredoxin-4	1.78	1.50e-4	782	Q13162	31	5,9	8	27	1,10E-03	
Structural function										
Villin 1	-1.4	1.93e-4	144	P09327	93	5,9	30	29	3,20E-14	
Lamin-A/C	2.25	1.93e-4	221	P02545	74	6,6	28	42	1,30E-12	
	2.3	5.12e-5	229				22	36	4,10E-08	
Actin beta	-2.55	2.79e-3	522	P60709	40	5,5	17	43	4,10E-13	
Actin-related protein 2/3 complex subunit 2	-1.64	2.06e-6	697	O15144	34	6,8	16	34	6,30E-08	
Purine metabolism										
Guanine deaminase	-1.27	4.58e-4	451	Q9Y2T3	51	5,4	12	28	9,10E-04	
Adenosine deaminase	-1.9	1.25e-3	519	P00813	41	5,6	13	29	2,60E-07	
Purine nucleoside phosphorylase	-2.07	2.26e-4	701	P00491	32	6,5	13	35	2,00E-06	
Other proteins										
Calcium-activated chloride channel regulator 1	-2.47	3.22e-4	169	A8K714	101	5,9	17	14	1,60E-08	
Voltage-dependent anion-selective channel protein 1	-1.46	8.48e-5	666	P21796	31	8,6	8	31	1,10E-04	
DnaJ homolog subfamily B member 11	1.31	7.56e-5	534	Q9UBS4	41	5,8	10	28	7,00E-05	

^aStandardized volume ratio of the protein spot, calculated by DeCyder BVA module, between Group B (CD patients with Marsh II-III) and Group A (controls and CD patients with Marsh 0-I) patients.

^b† Test P value determined by DeCyder EDA analysis.

^cSpot numbers referring to (30).

^dProtein accession numbers were derived from UniProtKB/Swiss-Prot database.

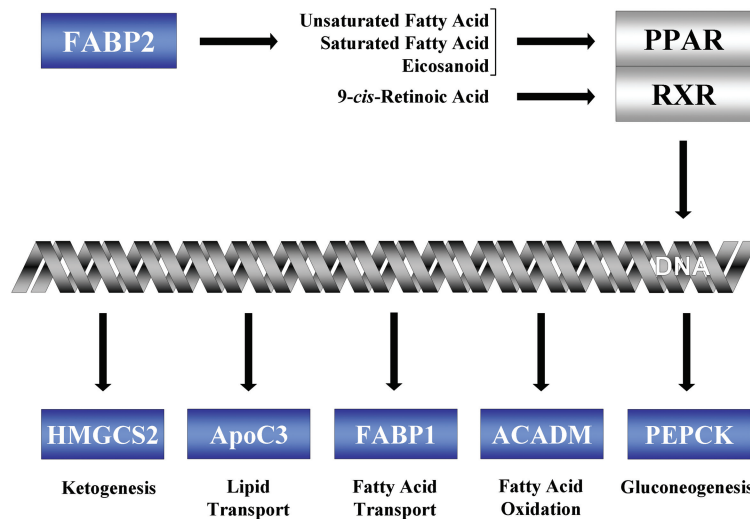


Figure 2. A simplified view of differentially expressed proteins according to PPAR signaling pathway resulting from Pathway Express tool analysis. All the illustrated proteins were downregulated in Group B (CD patients with Marsh II-III) with respect to Group A (Controls and CD patients with Marsh 0-I). Protein abbreviations correspond to Entrez Gene official symbols.

sents the best hallmark of CD patients with Marsh II-III. An enhanced local IgM secretion had already been demonstrated in CD patients (37). Since IgM antibodies can activate complement, it has been suggested that they might contribute to the damage following the encounter with antigens (for example, gluten) (38,39). Thus, our data confirm the concept of an IgM segregation in the gut, and indicate that B cells, responsible for IgM production, are associated with CD and are involved in tissue damage.

Two other proteins included in the classifiers, FABP1 and HMGCS2, are both integrated in the PPAR signaling pathway (40,41). Downregulation of PPAR signaling pathway in the highest grade of CD also is corroborated by the modulation of other proteins involved in PPAR signaling as FABP2, PEPCK, APOC3 and ACADM (see Figure 2) (Table 3) (42). Moreover, in the intestine, the PPAR ex-

Table 4. Marker selection results.^a

Spot number	Rank	Appearance	Name	Accession number
227	1	5	Immunoglobulin M	P01871
222	2	1	NI	NI
436	2	1	Hydroxymethylglutaryl-CoA synthase	P54868
1123	2	2	Fatty acid binding protein	P07148
134	2	1	Elongation factor 2	P13639

^aMarker selection calculation was performed with the set, including proteins present in more than 80% of spot maps and with a *t* test ($P < 0.05$). Analysis was performed with partial least squares method as the search method, and with regularized discriminant analysis as the evaluation method. As cross-validation options, we set five folds. In this table, we indicated the spot number, the rank value (the mean of the classifier's ranking of the protein), the appearance value (indicating the number of classifiers that have selected the corresponding protein), the protein name and the accession number from Swiss-Prot database. Owing to the low protein amount, we were not able to identify spot 222.

pression correlates with the abundance of the cellular retinol binding protein (42), that we found downregulated accordingly in Group B. Also carbonyl reductase (CBR1), known to be involved in the conversion of prostaglandin E2 (PGE₂) into PGF_{2 α} , and whose expression has been found to be induced as a consequence of PPAR α activation (43), was downregulated in Group B.

The PPAR α , γ and β/δ are ligand-activated nuclear receptors with a wide range of effects on metabolism, cellular proliferation, differentiation and immune response (44). They form heterodimers with the retinoid X receptor (RXR) and activate transcription by binding to specific DNA elements (see Figure 2) (44–46). PPARs are the major regulators of lipid and fatty acid metabolism and regulate transport, oxidation, storage and synthesis of fatty acids (47). Moreover PPAR γ activation increases glucose uptake and synthesis by skeletal muscle, and, in addition, reduces hepatic glucose production and its subsequent release by a decreased gluconeogenesis (48–50). Thus, the downregulation of PPAR pathway we found in the Marsh II and III CD could contribute to the downregulation of proteins involved in fatty acid and sugar metabolism observed in our and other series of CD patients (Table 3) (51).

Interestingly, a recent study has evidenced the correlation among gliadin,

tissue transglutaminase (TG2) and PPAR (52). The authors demonstrated that peptide p 31-43, one of the most “toxic” gliadin peptides for predisposed individuals (53), determined an increased production of reactive oxygen species and a TG2 overexpression in epithelial cells, which then induced PPAR γ ubiquitination and degradation (52). These findings are in line with our results evidencing that the proteins related to PPAR-signaling are downregulated. Moreover these data are particularly suggestive if we consider our preliminary results on RF-CD: in refractory. In RF-CD, where IgA-tTg mostly return to normal values, immunoblotting findings highlight a normalization of FABP level that is directly linked to PPAR level.

PPARs also are important regulators of the immune system. Recent data reported that a depressed expression or activity of these receptors might lead to an inability to mount an effective immune response and, possibly, to an exacerbation of autoimmune disease (54). Moreover, ligands for PPAR have therapeutic activity in several rodent models of inflammatory and autoimmune disease (45,55–57), thus suggesting that they might have similar effects in human disease as well. Besides, it has been shown that PPAR γ can inhibit the production of several T-cell cytokines, including the classical TH1-cell cytokine IFN- γ (58),

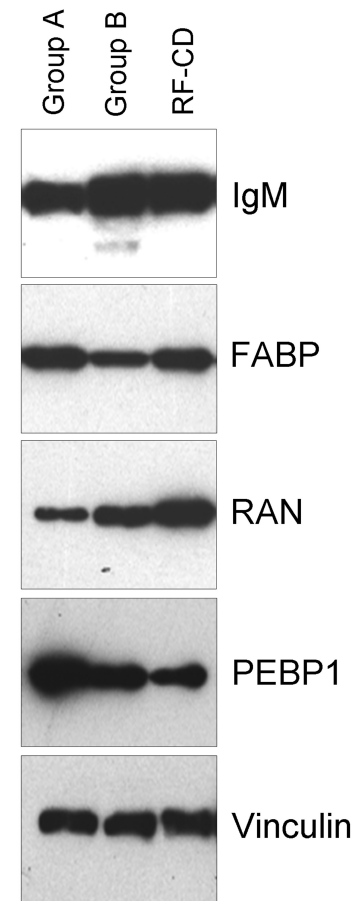


Figure 3. Validation by immunoblotting of several proteins differentially expressed in Group A compared with Group B and analysis of IGM, FABP, RAN and PEBP1 expression levels in RF-CD patients. Immunoblotting assay evidences the differential expression of IGM, FABP, RAN and PEBP1 in Group A (lane 1), Group B (lane 2) and in RF-CD patients (lane 3). Vinculin has been used as control for equal loading. Immunoblotting demonstrates the up-regulation of IgM and RAN and the down-regulation of the PEBP1 and FABP, in Group B compared with Group A, in accordance with the results obtained by 2D-DIGE analysis. In patients with RF-CD, IgMs remained elevated, FABP was reversed toward normalization, RAN was increased while PEBP1 was decreased with respect to both Group A and Group B CD patients. The Figure shows the results of three representative samples, one from each analyzed Group (A, B and RF-CD). Experimental details are described in the materials and method section.

known to be important in the maintenance of inflammation and in CD pathogenesis (11). These functions are mediated largely through the abilities of the PPAR α and γ to transrepress the activities of many inflammation-associated transcription factors, including NF- κ B (59). In fact, PPAR α can directly bind NF- κ B p65, thus interfering with NF- κ B transcriptional activation (45,60), while PPAR γ haploinsufficiency results in dysregulation of NF- κ B and hyperreactivity of B cells (54). Since NF- κ B is constitutively active in intestinal mucosa of patients with untreated CD (61), and autoantibodies are implicated in CD pathogenesis, we hypothesize that the downregulation of PPAR signaling pathway may contribute to the NF- κ B activation and play a pivotal role in the CD-associated inflammation. A further contribution to NF- κ B activation also is determined by the upregulation of RAN protein (62) and of PRDX4 (63), and by the downregulation of PEBP1, also known as RKIP (64,65), all of which we found modulated in our series (Table 3).

It is known that adult CD patients present a higher risk of developing cancer than the general population (4,5). In our series, we found the upregulation of known cancer-related proteins (RAN and PRDX4) (62,63) and the downregulation of PEBP1 (65). The Ran-GTP signaling pathway was found to be exploited preferentially in cancer (66), as becoming essential for cell division in transformed cells (but not in normal cells). In this regard, we reported a parallel increase in the RAN abundance and the Marsh index in CD previously (67). PRDX4 is an immediate regulator of H₂O₂-mediated NF- κ B activation (63); moreover it has been recently demonstrated that TNF-related apoptosis-inducing ligand (TRAIL), by suppressing the PRDX4 level, might facilitate cell death (68). PEBP1, also known as RKIP, is a modulator of the RAF/MAPK signaling cascade and acts as a suppressor of metastasis and apoptosis, and it was found downregulated in Group B (64).

Interestingly, if we consider our preliminary results on RF-CD, the proteins

associated with tumor development (RAN and PEBP1) (see Figure 3) continue to vary with respect to both Group A and Group B patients in a trend suggestive of an increased risk of malignant evolution.

As a whole, these results give an insight into the molecular mechanisms determining the perpetuation of the severe inflammatory response in CD and of the proteins possibly involved in cell deregulation associated with a risk to develop cancer.

Finally, our data suggest the potential role of PPAR as a therapeutic target for the modulation of inflammation in CD. The role of PPAR and the regulators of the inflammatory response in CD deserves further research focus.

ACKNOWLEDGMENTS

The authors wish to thank the “Centro di Biomedicina Molecolare” (CBM), which provided the Proteomic Instruments, and Anna Vallerugo for her writing assistance. This study was supported by Programma Integrato Oncologia, Tematica 2 and “Progetto celiachia complicata” Associazione Italiana Celiaci (AIC).

DISCLOSURE

The authors declare that they have no competing interests as defined by *Molecular Medicine*, or other interests that might be perceived to influence the results and discussion reported in this paper.

REFERENCES

- Marsh MN, Crowe PT. (1995) Morphology of the mucosal lesion in gluten sensitivity. *Baillieres Clin. Gastroenterol.* 9:273–93.
- Oberhuber G, Granditsch G, Vogelsang H. (1999) The histopathology of coeliac disease: Time for a standardized report scheme for pathologists. *Eur. J. Gastroenterol. Hepatol.* 11:1185–94.
- Catassi C, Fabiani E. (1997) The spectrum of coeliac disease in children. *Baillieres Clin. Gastroenterol.* 11:485–507.
- Cellier C, et al. (2000) Refractory sprue, coeliac disease, and enteropathy-associated T-cell lymphoma. French coeliac disease study group. *Lancet.* 356:203–8.
- Rampertab SD, Forde KA, Green PH. (2003) Small bowel neoplasia in coeliac disease. *Gut.* 52:1211–4.

- Green PH, Cellier C. (2007) Celiac disease. *N. Engl. J. Med.* 357:1731–43.
- Carmack SW, Lash RH, Gulizia JM, Genta RM. (2009) Lymphocytic disorders of the gastrointestinal tract: A review for the practicing pathologist. *Adv. Anat. Pathol.* 16:290–306.
- Catassi C, et al. (1994) Coeliac disease in the year 2000: Exploring the iceberg. *Lancet.* 343:200–3.
- Di Sabatino A, Corazza GR. (2009) Coeliac disease. *Lancet.* 373:1480–93.
- Sollid LM. (2002) Coeliac disease: Dissecting a complex inflammatory disorder. *Nat. Rev. Immunol.* 2:647–55.
- Nilsen EM, et al. (1998) Gluten induces an intestinal cytokine response strongly dominated by interferon gamma in patients with celiac disease. *Gastroenterology.* 115:551–63.
- Molberg O, et al. (1998) Tissue transglutaminase selectively modifies gliadin peptides that are recognized by gut-derived T cells in celiac disease. *Nat. Med.* 4:713–7.
- Camarca A, et al. (2009) Intestinal T cell responses to gluten peptides are largely heterogeneous: Implications for a peptide-based therapy in celiac disease. *J. Immunol.* 182:4158–66.
- Mohamed BM, et al. (2006) Increased protein expression of matrix metalloproteinases -1, -3, and -9 and TIMP-1 in patients with gluten-sensitive enteropathy. *Dig. Dis. Sci.* 51:1862–8.
- Mention JJ, et al. (2003) Interleukin 15: A key to disrupted intraepithelial lymphocyte homeostasis and lymphomagenesis in celiac disease. *Gastroenterology.* 125:730–45.
- Zhang X, Sun S, Hwang I, Tough DF, Sprent J. (1998) Potent and selective stimulation of memory-phenotype CD8+ T cells in vivo by IL-15. *Immunity.* 8:591–9.
- Meresse B, et al. (2004) Coordinated induction by IL15 of a TCR-independent NKG2D signaling pathway converts CTL into lymphokine-activated killer cells in celiac disease. *Immunity.* 21:357–66.
- Hue S, et al. (2004) A direct role for NKG2D/MICA interaction in villous atrophy during celiac disease. *Immunity.* 21:367–77.
- van Heel DA, et al. (2007) A genome-wide association study for celiac disease identifies risk variants in the region harboring IL2 and IL21. *Nat. Genet.* 39:827–9.
- Glas J, et al. (2009) Novel genetic risk markers for ulcerative colitis in the IL2/IL21 region are in epistasis with IL23R and suggest a common genetic background for ulcerative colitis and celiac disease. *Am. J. Gastroenterol.* 104:1737–44.
- Parrish-Novak J, et al. (2000) Interleukin 21 and its receptor are involved in NK cell expansion and regulation of lymphocyte function. *Nature.* 408:57–63.
- Dienz O, et al. (2009) The induction of antibody production by IL-6 is indirectly mediated by IL-21 produced by CD4+ T cells. *J. Exp. Med.* 206:69–78.
- Kuramitsu Y, Nakamura K. (2006) Proteomic analysis of cancer tissues: Shedding light on carcinogenesis and possible biomarkers. *Proteomics.* 6:5650–61.

24. Jiang YJ, Sun Q, Fang XS, Wang X. (2009) Comparative mitochondrial proteomic analysis of raji cells exposed to adriamycin. *Mol. Med.* 15:173–82.
25. De Re V, et al. (2007) Genetic insights into the disease mechanisms of type II mixed cryoglobulinemia induced by hepatitis C virus. *Dig. Liver Dis.* 39 Suppl 1:S65–71.
26. De Re V, et al. (2007) Proteins specifically hyperexpressed in a coeliac disease patient with aberrant T cells. *Clin. Exp. Immunol.* 148:402–9.
27. De Re V, et al. (2008) HCV inhibits antigen processing and presentation and induces oxidative stress response in gastric mucosa. *Proteomics Clin. Appl.* 2:1290–9.
28. Draghici S, et al. (2007) A systems biology approach for pathway level analysis. *Genome Res.* 17:1537–45.
29. De Re V, et al. (2006) HCV-NS3 and IgG-fc cross-reactive IgM in patients with type II mixed cryoglobulinemia and B-cell clonal proliferations. *Leukemia.* 20:1145–54.
30. Simula MP, et al. (2009) Two-dimensional gel proteome reference map of human small intestine. *Proteome Sci.* 7:10.
31. West J, et al. (2003) Seroprevalence, correlates, and characteristics of undetected coeliac disease in England. *Gut.* 52:960–5.
32. Fasano A, et al. (2003) Prevalence of coeliac disease in at-risk and not-at-risk groups in the United States: A large multicenter study. *Arch. Intern. Med.* 163:286–92.
33. Marsh MN. (1992) Gluten, major histocompatibility complex, and the small intestine. A molecular and immunobiologic approach to the spectrum of gluten sensitivity ('celiac sprue'). *Gastroenterology.* 102:330–54.
34. Memeo L, et al. (2005) Duodenal intraepithelial lymphocytosis with normal villous architecture: Common occurrence in H. pylori gastritis. *Mod. Pathol.* 18:1134–44.
35. Dickson BC, Streutker CJ, Chetty R. (2006) Coeliac disease: An update for pathologists. *J. Clin. Pathol.* 59:1008–16.
36. Briani C, Samaroo D, Alaedini A. (2008) Coeliac disease: From gluten to autoimmunity. *Autoimmun. Rev.* 7:644–50.
37. Crabtree JE, Heatley RV, Losowsky ML. (1989) Immunoglobulin secretion by isolated intestinal lymphocytes: Spontaneous production and T-cell regulation in normal small intestine and in patients with coeliac disease. *Gut.* 30:347–54.
38. Scott BB, Scott DG, Losowsky MS. (1977) Jejunal mucosal immunoglobulins and complement in untreated coeliac disease. *J. Pathol.* 121:219–23.
39. Halstensen TS, Hvatum M, Scott H, Fausa O, Brandtzaeg P. (1992) Association of subepithelial deposition of activated complement and immunoglobulin G and M response to gluten in coeliac disease. *Gastroenterology.* 102:751–9.
40. Kaikaus RM, Chan WK, Ortiz de Montellano PR, Bass NM. (1993) Mechanisms of regulation of liver fatty acid-binding protein. *Mol. Cell. Biochem.* 123:93–100.
41. Juge-Aubry C, et al. (1997) DNA binding properties of peroxisome proliferator-activated receptor subtypes on various natural peroxisome proliferator response elements. Importance of the 5'-flanking region. *J. Biol. Chem.* 272:25252–9.
42. Desvergne B, Wahli W. (1999) Peroxisome proliferator-activated receptors: Nuclear control of metabolism. *Endocr. Rev.* 20:649–88.
43. Yokoyama Y, et al. (2007) Clofibrilic acid, a peroxisome proliferator-activated receptor alpha ligand, inhibits growth of human ovarian cancer. *Mol. Cancer. Ther.* 6:1379–86.
44. Kota BP, Huang TH, Roufogalis BD. (2005) An overview on biological mechanisms of PPARs. *Pharmacol. Res.* 51:85–94.
45. Straus DS, Glass CK. (2007) Anti-inflammatory actions of PPAR ligands: New insights on cellular and molecular mechanisms. *Trends Immunol.* 28:551–8.
46. Delerive P, Fruchart JC, Staels B. (2001) Peroxisome proliferator-activated receptors in inflammation control. *J. Endocrinol.* 169:453–9.
47. Kersten S, Desvergne B, Wahli W. (2000) Roles of PPARs in health and disease. *Nature.* 405:421–4.
48. Zierath JR, et al. (1998) Role of skeletal muscle in thiazolidinedione insulin sensitizer (PPARgamma agonist) action. *Endocrinology.* 139:5034–41.
49. Raman P, Judd RL. (2000) Role of glucose and insulin in thiazolidinedione-induced alterations in hepatic gluconeogenesis. *Eur. J. Pharmacol.* 409:19–29.
50. Bragt MC, Popeijus HE. (2008) Peroxisome proliferator-activated receptors and the metabolic syndrome. *Physiol. Behav.* 94:187–97.
51. Bertini I, et al. (2009) The metabonomic signature of coeliac disease. *J. Proteome Res.* 8:170–7.
52. Maiuri L, et al. (2010) Lysosomal accumulation of gliadin p31–43 peptide induces oxidative stress and tissue transglutaminase-mediated PPARgamma downregulation in intestinal epithelial cells and coeliac mucosa. *Gut.* 59:311–9.
53. Maiuri L, et al. (2003) Association between innate response to gliadin and activation of pathogenic T cells in coeliac disease. *Lancet.* 362:30–7.
54. Setoguchi K, et al. (2001) Peroxisome proliferator-activated receptor-gamma haploinsufficiency enhances B cell proliferative responses and exacerbates experimentally induced arthritis. *J. Clin. Invest.* 108:1667–75.
55. Kielian T, Drew PD. (2003) Effects of peroxisome proliferator-activated receptor-gamma agonists on central nervous system inflammation. *J. Neurosci. Res.* 71:315–25.
56. Lovett-Racke AE, et al. (2004) Peroxisome proliferator-activated receptor alpha agonists as therapy for autoimmune disease. *J. Immunol.* 172:5790–8.
57. Dubuquoy L, et al. (2006) PPARgamma as a new therapeutic target in inflammatory bowel diseases. *Gut.* 55:1341–9.
58. Cunard R, et al. (2002) Regulation of cytokine expression by ligands of peroxisome proliferator activated receptors. *J. Immunol.* 168:2795–802.
59. Daynes RA, Jones DC. (2002) Emerging roles of PPARs in inflammation and immunity. *Nat. Rev. Immunol.* 2:748–59.
60. Delerive P, et al. (1999) Peroxisome proliferator-activated receptor alpha negatively regulates the vascular inflammatory gene response by negative cross-talk with transcription factors NF-kappaB and AP-1. *J. Biol. Chem.* 274:32048–54.
61. Maiuri MC, et al. (2003) Nuclear factor kappa B is activated in small intestinal mucosa of coeliac patients. *J. Mol. Med.* 81:373–9.
62. Jiang X, et al. (2003) NF-kappa B p65 transactivation domain is involved in the NF-kappa B-inducing kinase pathway. *Biochem. Biophys. Res. Commun.* 301:583–90.
63. Jin DY, Chae HZ, Rhee SG, Jeang KT. (1997) Regulatory role for a novel human thioredoxin peroxidase in NF-kappaB activation. *J. Biol. Chem.* 272:30952–61.
64. Odabaei G, et al. (2004) Raf-1 kinase inhibitor protein: Structure, function, regulation of cell signaling, and pivotal role in apoptosis. *Adv. Cancer Res.* 91:169–200.
65. Yeung KC, et al. (2001) Raf kinase inhibitor protein interacts with NF-kappaB-inducing kinase and TAK1 and inhibits NF-kappaB activation. *Mol. Cell. Biol.* 21:7207–17.
66. Xia F, Lee CW, Altieri DC. (2008) Tumor cell dependence on ran-GTP-directed mitosis. *Cancer Res.* 68:1826–33.
67. Simula MP, et al. (2009) Comment re: Ran-GTP control of tumor cell mitosis. *Cancer Res.* 69:1240; author reply 1240.
68. Wang H, et al. (2009) TNF-related apoptosis-inducing ligand suppresses PRDX4 expression. *FEBS Lett.* 583:1511–5.